Article

Alloying Effects on the Stability of D0$_{22}$ γ″-Ni$_3$M (M: Nb, Ta, V) Precipitates at Elevated Temperatures in Alloy 718 Type Ni-Based Alloys

Kako Tokutomi, Kyosuke Sagitani and Satoru Kobayashi *

Department of Materials Science and Engineering, Tokyo Institute of Technology, 2-12-1 Ookayama Meguro-ku, Tokyo 152-8552, Japan; kako.t.bbsj@gmail.com (K.T.); sagitani.k.tokyo.tech@gmail.com (K.S.)
* Correspondence: kobayashi.s.be@m.titech.ac.jp

Abstract: The effects of alloying elements, M (M = Nb, Ta, and V), on the stability of D0$_{22}$ γ″-Ni$_3$M precipitates at elevated temperatures were investigated in Ni-22Cr-based ternary and quaternary alloys using heat-treated diffusion-multiple and bulk samples with discrete chemical compositions, with a final goal to improve the precipitate stability and the temperature capability of the Alloy-718-type Ni-based superalloys. Our microstructural characterization indicated that a complete replacement of Nb with Ta stabilized the γ″ precipitates at temperatures up to 800 °C. A partial replacement of Ta with V was found to stabilize the precipitates even at 900 °C. Differential scanning calorimetry and high-temperature X-ray diffraction experiments demonstrated that the D0$_a$-Ni$_3$M structure was stable at elevated temperatures in the Ni-Cr-Ta ternary system. Lattice parameter measurements at room temperature suggested that a partial replacement of Ta with V decreased the lattice misfit between the fcc γ matrix and the γ″ precipitate phases along the *a*- and *c*-axes of the tetragonal γ″ crystal structure. The improved γ″ precipitate stability was discussed in terms of the chemical driving force, misfit strain, and diffusion kinetics viewpoints.

Keywords: microstructural stability; metastable phase; Ni-based wrought alloys

1. Introduction

Alloy 718 is an important class of Nb-bearing Ni-based superalloys for high-temperature applications, such as compressor disks/blades and turbine disks in gas turbine systems for land-based power plants and aerospace engines, due to their high strength/toughness and good fabricability [1]. Improvements in the efficiency of gas turbine systems allow us to reduce energy consumption and CO$_2$ emissions, and an increase in the heat resistance of the high-temperature components is, accordingly, a continuously important subject.

The strength of Alloy 718 is derived from a fine/coherent precipitation of thermodynamically metastable D0$_{22}$ γ″-Ni$_3$Nb precipitates in the fcc γ–Ni matrix [2]. The metastable feature of the γ″ precipitates, however, causes phase transformations from their structure to the thermodynamically stable D0a δ-Ni$_3$Nb structure at elevated temperatures. This results in the formation of a coarse microstructure, the degradation of mechanical properties, thereby limiting the service temperature of the alloys below ~650 °C [3–5]. Improvements in the γ″ precipitate stability would, therefore, be expected to enhance the heat resistance of the Alloy-718-type Ni-based superalloys. Developments for this purpose have been tried by increasing the ratio of Al/Nb to optimize the volume fraction of the γ″-Ni$_3$Nb phase and the γ′-Ni$_3$Al phase [5–7].

Aiming at improving the stability of the γ″ phase itself, we focused on the substitution of Nb with other γ″-forming elements, and preliminarily found that a replacement of Nb with Ta drastically retarded the phase transformation from γ″ to δ at 800 °C in Ni-22Cr-based ternary alloys. The same trend was reported in a previous study [8] by the

substitution of Ta for Nb in an Alloy 718 chemical composition. However, the reason for the improved stability has not been clarified yet.

In the Ni-Ta binary alloy system, the Pt_3Nb-type structure (β) has been reported as thermodynamically stable as a Ni_3Ta-based intermetallic compound, while the $D0_{22}$- and the $D0_a$-type structures are metastable [9]. A phase transition from the β phase to the $D0_{22}$ on heating was reported [10]. The latter report could suggest that the γ'' phase is thermodynamically stable at elevated temperatures in the Ni-Ta alloys, but this point needs to be verified. The $D0_{22}$ γ''-Ni_3V phase is, on the other hand, known to exist as a thermodynamically stable intermetallic phase in the Ni-V binary alloy system [9], which suggests that a replacement of Nb and/or Ta with V could improve the γ'' precipitates by increasing their relative thermodynamic stability with regard to the other structures.

It is generally considered that misfit strains, due to coherency at the matrix/precipitate interfaces, drive phase transformations, including those from a metastable phase to their stable phase [11–13]. The γ''-Ni_3Nb phase precipitates coherently in the matrix in a disk shape typically with its lattice parameter being larger than the γ–Ni matrix phase by less than 0.1% along the *a*-axis and by 3~5% along the *c*-axis of the γ'' crystal structure [11,12,14]. Those relatively large misfit strains could also be an important factor for controlling the stability of γ'' precipitates at elevated temperatures. The *a*-axis and the *c*-axis of the γ'' phase are reported to be shorter in Ni_3V than in Ni_3Nb and Ni_3Ta [9,15]. A replacement of Nb and/or Ta with V could, thus, allow us to expect a change in the misfit strain energy, thereby modifying the driving force for the phase transformation.

In the present paper, the stability of $D0_{22}$ γ''-Ni_3M (M: Nb, Ta, and V) precipitates at elevated temperatures was investigated by varying the ratio of the γ''-forming elements M in Ni-22Cr-based ternary and quaternary alloys. The obtained results were discussed in terms of the chemical driving force, misfit strain, and diffusion kinetics viewpoints.

2. Materials and Methods

The investigation was conducted using a diffusion-multiple method [16–19] and a conventional bulk alloy method. In the diffusion-multiple method adopted, a diffusion multiple was firstly heat-treated at an elevated temperature to introduce concentration gradients of solute elements in a matrix phase and then annealed to cause a precipitation reaction in the matrix phase with concentration gradients, which could provide us with an effective microstructural characterization sample. Three alloy end members were coupled in the present study, of which nominal compositions and designations are listed in Table 1. Their chemical compositions are shown in atomic percent through this paper unless specified. The chemical compositions of each end member were selected in such a way that each γ''-phase-forming element was soluble in the γ matrix in the first heat treatment and was precipitated as Ni_3M intermetallic compound phases in the second heat treatment.

Table 1. The chemical compositions of the alloys used in the present study.

Sample	Alloy	Alloy Composition (at.%)				
Type	Designation	Nb	Ta	V	Cr	Ni
DM	5.5Nb	5.5	-	-	22.0	Bal.
DM	6.5Ta	-	6.5	-	22.0	Bal.
DM	10V	-	-	10.0	22.0	Bal.
B	3.7Ta	-	3.7	-	24.7	Bal.
B	3Ta-5V	-	3.0	5.0	22.0	Bal.
B	6Ta-5V	-	6.0	5.0	22.0	Bal.
B	20.4Ta	-	20.4	-	5.4	Bal.

DM: diffusion-multiple samples; B: bulk alloy samples.

The end members were prepared with argon arc melting using 3 N purity pure raw metal materials in the form of 30 g button ingots, cold rolling, and machining. Diffusion

bonding surfaces of the end members were ground and, finally, polished down to 3 mm diamond polishing suspension. The end members were cleaned with ethanol, coupled in a molybdenum tube, and heat-treated at 1200 °C for 169 h to introduce continuous composition gradients of the γ''-forming elements in the γ matrix through the interdiffusion of the elements. The diffusion multiple was, subsequently, aged at 800 °C and 900 °C for time periods of up to 2000 h to determine the stability of γ'' precipitates within the matrix phase. The samples were sectioned perpendicular to the diffusion-bonded interfaces before and after the second heat treatment. The sections were mechanically polished down to 0.5 μm Al_2O_3 polishing suspension, chemically polished with SiO_2 polishing suspension, and used for metallographic observations and chemical analysis.

The microstructures of the heat-treated samples were observed with an optical microscope (OM) and a field-emission-type high-resolution scanning electron microscope (FESEM, JSM-7000F, JEOL Ltd., Tokyo, Japan) equipped with a backscattered electron (BSE) detector. The chemical analysis was conducted along lines across each diffusion-bonded interface in the diffusion-multiple samples. The chemical composition was analyzed with energy dispersive spectroscopy (EDS) on FESEM. The solute contents were quantified using calibration curves, which were prepared using alloys with known chemical compositions. The crystallographic orientation of the matrix phase was measured with electron backscatter diffraction (EBSD) on FESEM.

Bulk alloys, alloys of discrete chemical compositions, were also used for further investigation into the stability of γ'' precipitates. The chemical compositions and designations of the bulk alloys are listed in Table 1. The first three bulk alloys were fabricated to confirm the effect of a partial replacement of Ta with V, as explained in detail later. These bulk alloys were prepared with argon arc melting, cold-rolled, solution-treated, and aged under the conditions shown in Table 1. The metallographic samples of these alloys were prepared with the same method for diffusion-multiple samples. X-ray diffraction (XRD) was conducted at room temperature for phase identification and for evaluation of the lattice parameters of γ and γ'' phases. XRD was conducted with a machine (Mini Flex 600, Rigaku Corp., Tokyo, Japan) using Cu radiation and a Ni filter.

High-temperature X-ray diffraction (HTXRD) and differential scanning calorimetry (DSC) were performed for the identification of the phase transition with temperatures in the Ni_3Ta phase composition using the fourth bulk alloy in Table 1. HTXRD was conducted with a machine (D8 Discover mHR, Bruker AXS, Billerica, MA, USA) using Cu radiation and a collimator with a diameter of 0.5 mm with a heating stage (DHS-900, Anton Paar, Graz, Austria). DSC was conducted to detect a phase transition with a machine (DSC 404 Fe Pegasus, Netzsch, Burlington, MA, USA) in an argon atmosphere at a heating rate of 10 °C/min between room temperature and 900 °C.

3. Results and Discussion

3.1. Microstructures of Diffusion Multiples

Figure 1 shows an optical micrograph of a cross-section of the diffusion-multiple sample heat-treated at 1200 °C for 169 h and the concentration profiles taken along the line across the diffusion-bonded interface. It can be seen that the Ta and V concentrations gradually changed within the γ phase across the initial interface, while the Cr concentration remained almost constant. It was confirmed that all the solute elements were in a solid solution, and the precipitates were rarely detected using optical microscopy and FESEM observation. This heat-treated diffusion-multiple sample was, subsequently, aged to precipitate the γ''-phase-forming elements within the matrix with the concentration gradients.

BSE images taken from the diffusion-multiple samples aged at 800 °C are shown in Figure 2. In the 5.5Nb area (Figure 2a), discontinuously precipitated lamellar colonies were observed after aging for 100 h, indicating that metastable γ''-Ni_3Nb precipitates were already replaced by the thermodynamically stable δ-Ni_3Nb phase within the short time of aging. In the 6.5Ta area (Figure 2b), however, after aging for ~1000 h, fine γ'' precipitates were kept in half of the area of the diffusion couple sample, while discontinuously

precipitated lamellar colonies were formed in another half of the area. The γ″ precipitates in the grain were discriminated from the δ phase according to their habit planes and crystallographic orientation relationship: {100}$_\gamma$ // {001}$_{\gamma''}$, {111}$_\gamma$ // (010)$_\delta$ [12]. Our microstructural and chemical characterization indicated that the volume fraction of the coarse precipitates was ~22% in the 6.5Ta area, while that in the 5.5Nb area was ~20%. The similar volume fractions of the precipitates suggested that the improved stability of γ″ precipitates was due to the replacement of Nb with Ta rather than a lower volume fraction of precipitates, which would normally slow the precipitation kinetics. In the Ta/V interface area with a chemical composition of nearly Ni-22Cr-2.5Ta-5V, only γ″ precipitates were found in the matrix, although the density of the precipitates was lower than that of the precipitates observed in the 6.5Ta area (Figure 2c). In the 10V area (Figure 2d), fine precipitates with a grayish contrast were visible within the matrix. The darker contrast and the size of the precipitates allowed us to assume that the γ″-Ni$_3$V phase was precipitated during cooling after the second heat treatment. The particles with a black contrast, displayed in the V-containing areas, were assumed to be vanadium nitride caused by the inclusion of nitrogen in the raw material of V.
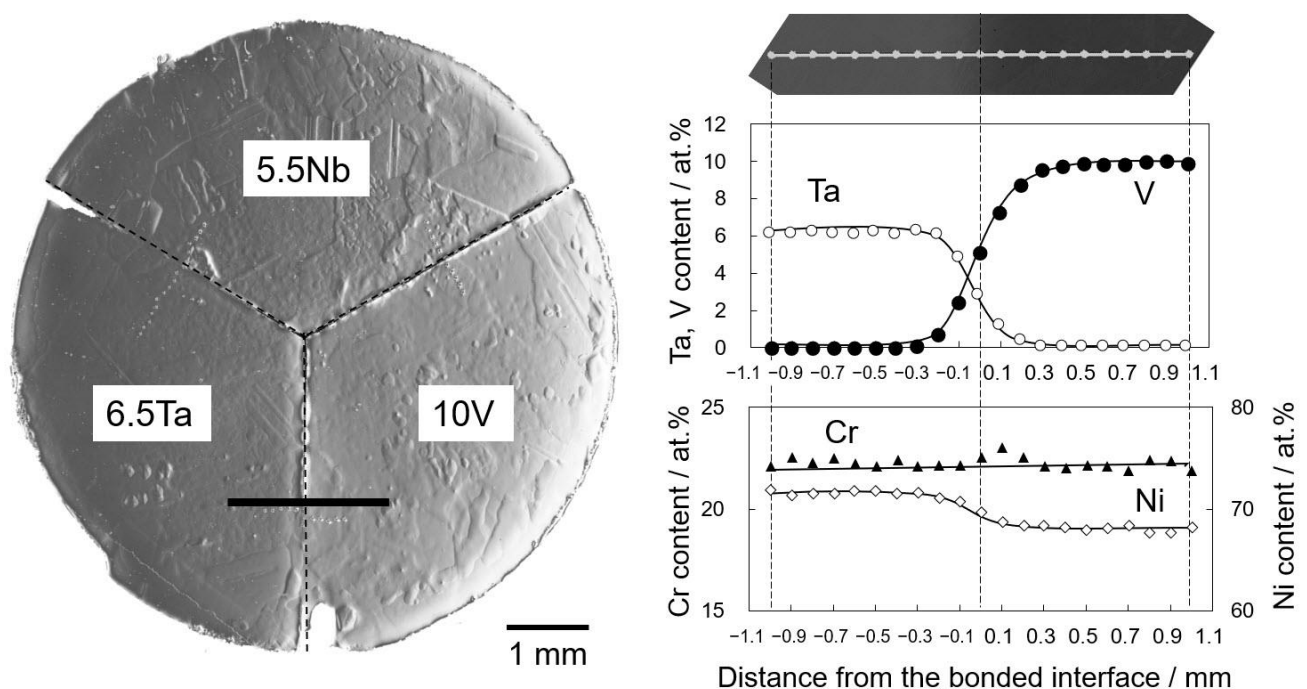

Figure 1. Optical micrograph of a diffusion-multiple sample heat-treated at 1200 °C for 169 h and compositional profiles across the 6.5Ta/10V diffusion-bonded interface.

Figure 3 shows BSE images taken from the diffusion-multiple samples aged at 900 °C. The entire portion of the 6.5Ta area was occupied by discontinuously precipitated lamellar colonies after 500 h (Figure 3a), which indicated that the γ″ precipitates were transformed into a stable phase. A Ta/V interface area with a chemical composition of Ni-22Cr-2Ta-5V showed lath-shaped precipitates with orthogonally aligned variants in the γ matrix even after 2000 h (Figure 3b). A trace analysis using EBSD suggested that the orthogonally aligned precipitates were of the γ″ phase according to the known crystallographic orientation relationship between the precipitate and the matrix phases: <100>$_\gamma$ // [001]$_{\gamma''}$ [12]. An example of the trace analysis to identify the γ″ phase is shown in Figure 3c.
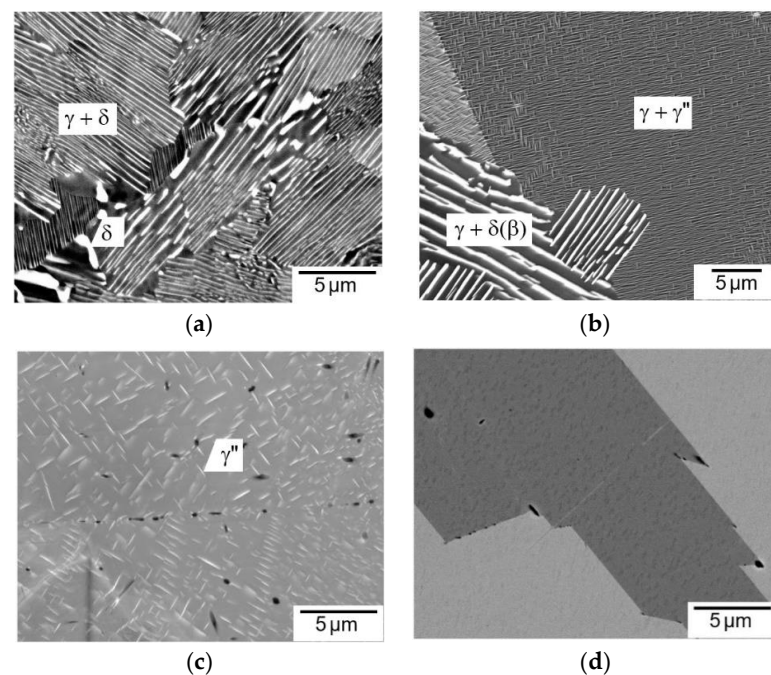
Figure 2. BSE images taken from diffusion-multiple samples aged at 800 °C for (**a**) 100 h in the 5.5Nb area, (**b**) 1026 h in the 6.5Ta area, (**c**) 1026 h in the vicinity of the 6.5Ta/10V diffusion-bonded interface, and (**d**) 1026 h in the 10V area. The precipitates in the micrographs were indexed by also taking the XRD results as shown in Section 3.2. into consideration. δ(β) denotes that the phase was of the δ phase at the aging temperature, but was transformed to the β phase during quenching.

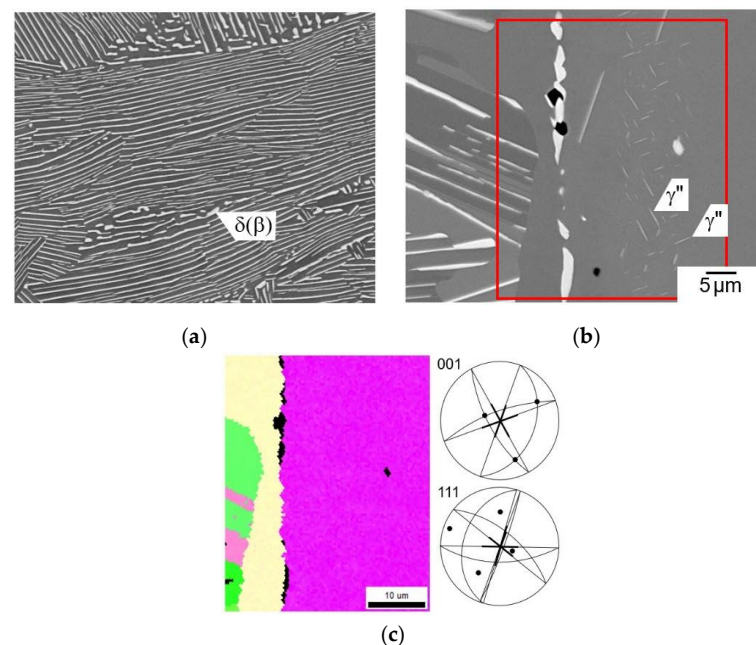**Figure 3.** BSE images taken from diffusion-multiple samples aged at 900 °C for (**a**) 500 h in the 6.5Ta area and (**b**) 2000 h in the vicinity of the 6.5Ta/10V diffusion-bonded interface. The right-bottom scale in (**b**) was common for the micrograph in (**a**). (**c**) EBSD IPF map of the matrix fcc phase taken from the designated red square area in (**b**), and trace analyses of (001) and (111) planes in the fcc matrix crystal with purple color. The precipitates along the (001) traces are γ″ phase, while those along the (111) traces are δ phase based on the reported crystallographic orientations [12]. The precipitate type in (**a**) was indexed according to the XRD results as shown in Sections 3.2 and 3.3.

3.2. Microstructures of Bulk Alloy Samples

The bulk alloys of three discrete alloy compositions were prepared to confirm the effect of the partial replacement of Ta with V on the stability of γ'' precipitates. The chemical compositions of the three alloys were designed to compare at the same volume fraction of the Ni_3M phase (V_f^{Ni3M}) in the presence/absence of vanadium, according to internal tie-line data at 900 °C. The V_f^{Ni3M} was ~6% in the 3.7Ta and the 3Ta-5V alloys. The V_f^{Ni3M} in the 6Ta-5V alloy was ~20%, almost equivalent to that in the 6.5Ta area in the diffusion multiple.

Figure 4a–d show BSE images of the alloys heat-treated at 900 °C for 500 h. The 3.7Ta alloy showed a small amount of globular-shaped precipitates on the grain boundaries and needle-shaped precipitates in the grain interior (Figure 4a). In the 3Ta-5V alloy (Figure 4b), orthogonally aligned fine precipitates were seen in the grain interiors together with globular- and needle-shaped coarse precipitates. In the alloys with higher V_f^{Ni3M}, while coarse lamella colonies were seen in the entire part of the 6.5Ta area (Figure 4c), not only coarse lamella colonies, but also fine lath-type precipitates were observed in the 6Ta-5V alloy (Figure 4d). Microstructures of the 3Ta-5V and the 6Ta-5V samples aged at 800 °C for 1000 h are displayed in Figure 4e,f. In both the samples, orthogonally aligned fine precipitates were observed in the grain interiors, together with discontinuously precipitated coarse lamellar colonies. The density of the fine precipitates in the 3Ta-5V sample (Figure 4e) was higher than that observed in a low Ta content area in the diffusion couple sample aged at a comparable condition (compare with Figure 2c), while the density in the 6Ta-5V sample (Figure 4f) was similar to that in the 6.5Ta area in the diffusion couple sample (compare with Figure 2b).
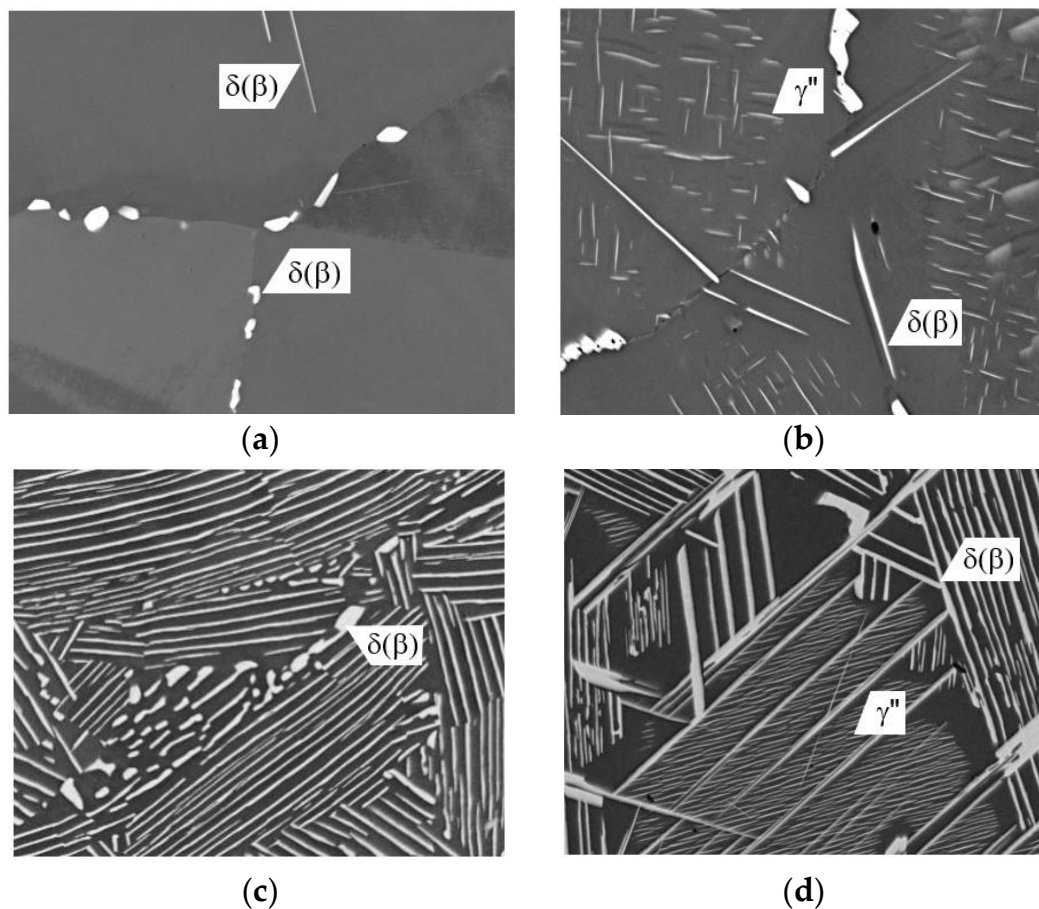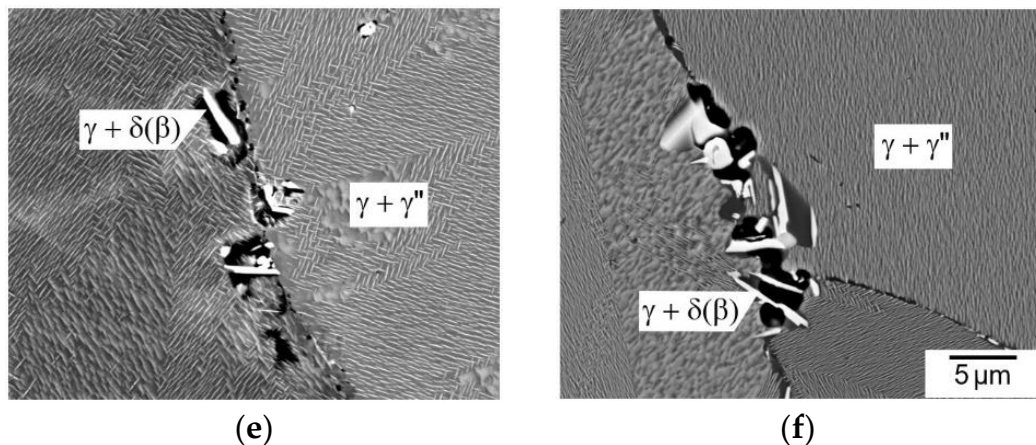

(a)

(b)

(c)

(d)

Figure 4. *Cont.*

Figure 4. BSE images of the samples aged at 900 °C for 500 h (**a–d**) and at 800 °C for 1000 h (**e,f**): (**a**) 3.7Ta, (**b,e**) 3Ta-5V, (**c**) 6.5Ta, (**d,f**) 6Ta-5V. The bottom-right scale was common for all the micrographs. The precipitates were indexed by taking into account the XRD results as shown in this section and Section 3.2.

Figure 5 shows room temperature XRD profiles obtained from the samples of which micrographs are presented in Figure 4a,b,d. In the 3.7Ta alloy (Figure 5a), the observed diffraction peaks were identified as γ-Ni (fcc) and β-Ni$_3$Ta with the Pt$_3$Nb structure [15]. In the 3Ta-5V and the 6Ta-5V alloys (Figure 5b,c), the diffracted peaks were identified as γ-Ni (fcc), γ''-Ni$_3$Ta, and β-Ni$_3$Ta. The precipitates were indexed in the micrographs in Figure 4 according to the XRD results. The precipitates in the diffusion-multiple samples were also assumed based on the bulk alloys and indexed in Figure 3. The comparison in the precipitate stability between the alloys clearly indicated that the partial replacements of Ta with V stabilized the γ'' precipitates even at 900 °C.
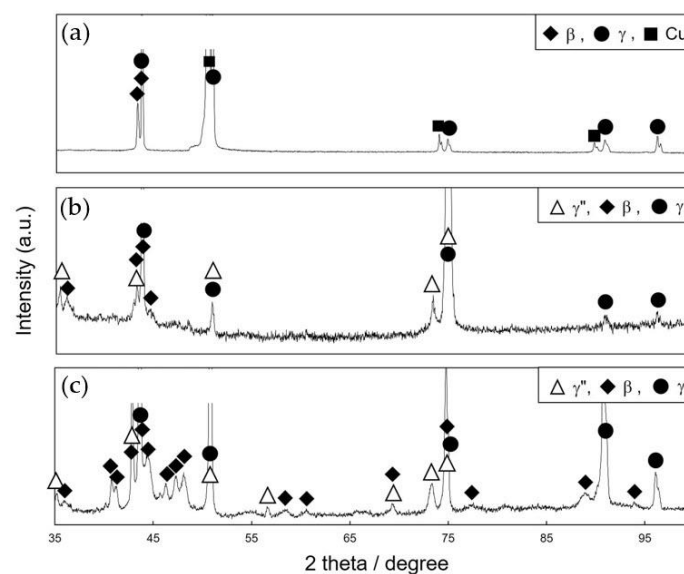

Figure 5. Room temperature XRD profiles obtained from the alloys aged at 900 °C for 500 h: (**a**) 3.7Ta, (**b**) 3Ta-5V, (**c**) 6Ta-5V. Cu peaks in (**a**) were derived from a Cu tape placed to cover phenol resin for sample mounting.

3.3. Chemical Driving Force Consideration

The change in the chemical driving force for the metastable→stable phase transformation was considered as one of the critical factors for the stability of γ'' precipitates at elevated temperatures. In the Ni-Ta binary alloy system, the Pt$_3$Nb-type structure (β) was

reported as thermodynamically stable at the Ni_3Ta phase, while the $D0_{22}$- and $D0_a$-type structures were metastable [9]. Fistov et al. [10] investigated the phase transformation in a Ni-25Ta alloy with DSC and HTXRD. They reported that the alloy showed a phase transition from the Pt_3Nb structure to the $D0_{22}$ structure at ~300 °C on heating. Their results could suggest that the γ'' phase was thermodynamically stable above 300 °C in the Ni-Ta alloys. To verify this, the β-Ni_3Ta precipitate was chemically analyzed in our aged samples, and an alloy with the analyzed composition, 20.4Ta alloy, was prepared for DSC and HTXRD measurements in the present study.

Figure 6 shows a DSC curve obtained from the 20.4Ta alloy sample. An endothermic peak was observed at ~380 °C, which reasonably corresponded to the phase transition reported in [10]. Figure 7 shows HTXRD profiles obtained at different temperatures from the 20.4Ta alloy. All the diffracted peaks were identified as the β-Ni_3Ta phase at room temperature within the measured 2θ angle range, except one peak at ~48.5°, which might be of the μ-NiTa phase ($D8_5$). The relative peak intensities were unchanged between room temperature and 300 °C (see Figure 7a–d). At 400 °C (Figure 7e), the diffracted peaks due to the δ-$D0_a$ crystal structure appeared. The intensities of the δ phase diffraction peaks increased, while those of the β phase decreased with an increase in temperature up to 600 °C (see Figure 7e–g). Any diffraction peaks due to the γ'' phase were not observed for all the temperatures measured. The results obtained from the DSC and HTXRD indicated that the δ phase was thermodynamically stable at elevated temperatures, where the stability of γ'' precipitates was investigated in the present study.
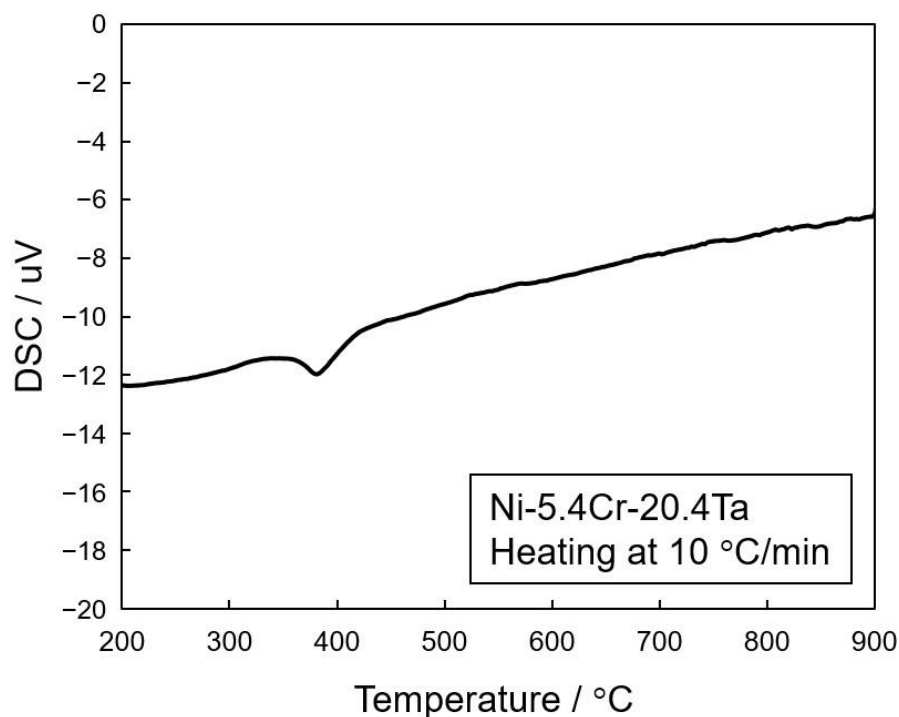

Figure 6. DSC curve obtained from the 20.4Ta alloy upon heating at a rate of 10 °C/min.

The heat of formation was calculated for the $D0_{22}$, β, and $D0_a$ type Ni_3Ta phases at absolute zero temperature based on the density function theory in the literature [20–22]. The calculated values were, however, in contradiction, i.e., the value was lower in $D0_{22}$ than $D0_a$ in [20,22], while the opposite order in values was reported in [21]. It was difficult to experimentally estimate the finite temperature free energy terms due to the metastability of the $D0_{22}$ phase. As far as the authors' knowledge goes, no theoretical study was available on the thermodynamic stability of the structures at finite temperatures in γ''-phase-forming Ni-based alloy systems, which was expected to be conducted in the future.
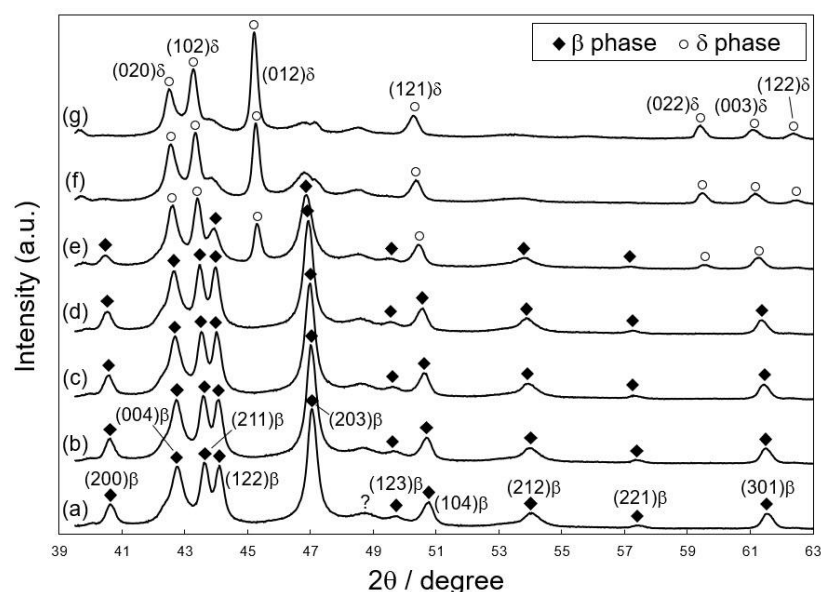
Figure 7. XRD profiles obtained from the 20.4Ta alloy at (**a**) room temperature, (**b**) 100 °C, (**c**) 200 °C, (**d**) 300 °C, (**e**) 400 °C, (**f**) 500 °C, and (**g**) 600 °C.

A partial replacement of Ta with V was expected to increase the thermodynamic stability of the γ″ phase with respect to the δ phase or the β phase, since the former structure was thermodynamically stable in the Ni-V binary alloy system [9]. The improved stability of γ″ precipitates could be, therefore, qualitatively interpreted in terms of an increased thermodynamic stability of the γ″ phase in the partially replaced alloys.

3.4. Misfit Strain Energy Consideration

It is generally considered that the misfit strain introduced by coherent precipitates drives phase transformations, including those from a metastable phase to their thermo-dynamically stable phase [13]. The γ″-Ni_3Nb phase precipitated coherently in the matrix in a disk shape, typically with its lattice parameter being larger than the γ–Ni matrix phase by less than 0.1% along the *a*-axis and by 3~5% along the *c*-axis of the γ″ crystal structure [11,12,14]. The relatively large misfit strain could also be an important factor in controlling the stability of γ″ precipitates at elevated temperatures.

Figure 8 shows a change with a partial replacement of Ta with V in the lattice misfit between the γ/γ″ phases along the *a*-axis and the *c*-axis of the γ″ structure. The values were derived through our XRD measurements at room temperature for the respective alloys and the reported crystallographic relationships [12,14]. The lattice parameters of the two phases were evaluated by selecting the peaks for the γ phase ((111), (200), (220), (311), and (222)) and the γ″ peaks that did not overlap with the γ phase ones (such as (110), (004), (202), (211), (114), (213), (204), (116), (224), (321), and (314)) without the deconvolution of the peaks using Cohen's error function method [23]. It can be seen that the lattice misfit values along both the axes decreased by the partial replacements. The observed decrease in the misfit was reasonable, since the *a*-axis and the *c*-axis of the γ″ Ni_3V phase were shorter than those of the γ″ Ni_3Ta [15]. The reduced lattice mismatch could allow us to assume that the driving force for the phase transformation was lowered, which could also be a qualitative interpretation for the improved stability of γ″ precipitates in the V-replaced alloys. The relative importance of the chemical driving force vs. misfit strain energy is an open question for future work. The misfit values measured in a 3.5 at.% Nb-doped alloy [14] are included in Figure 8. The value along the *c*-axis was similar to those in the 3.7Ta and 6.5Ta alloys, while the value along the *a*-axis was close to the alloys with the lower Ta contents, regardless of the presence of V. Taking into account that the addition of Fe slightly increased the misfit values, a comparison in the misfit values among the alloys

could not lead to any clear correlation between the misfit strain energy and the stability improvement by the substitution of Nb with Ta.
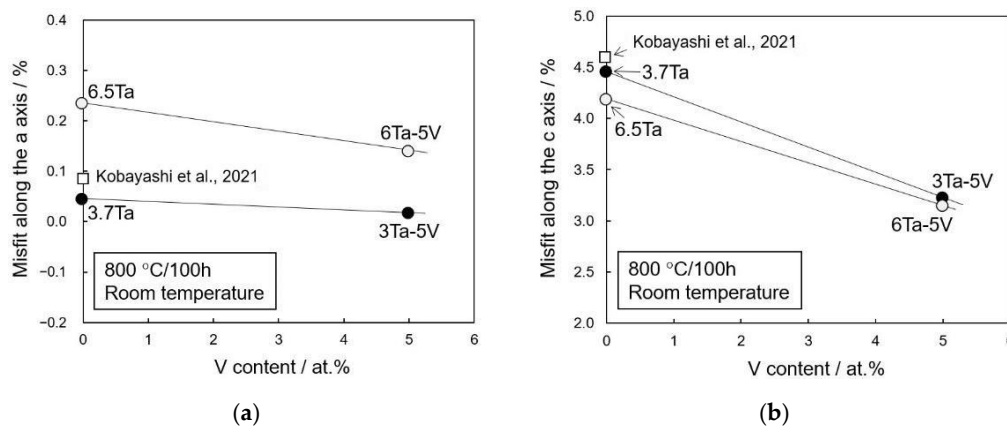

Figure 8. Estimated lattice misfit values between the γ and γ'' phases along the two axes of the tetragonal γ'' structure in the designated alloys: (**a**) along the *a*-axis and (**b**) along the *c*-axis. The misfit values were estimated from the lattice parameters of the corresponding phases measured with XRD at room temperature on the alloys aged at 800 °C for 100 h. The misfit values measured in a Nb-doped alloy (Ni-22Cr-16Fe-3.5Nb in at.%) [14] were also included.

3.5. Diffusion Kinetics Consideration

The changed stability of γ'' precipitates could be caused by the diffusion kinetics of the γ''-forming elements, since the phase transformation from γ'' to δ was diffusional. Figure 9 summarizes the reported diffusion coefficient of Nb [24,25], V [25,26], and Ta [25,27]. It can be seen that the coefficient of Nb reported in [24] was at most five times higher than that of Ta and V in the temperature range concerned, while the difference among the three elements was smaller in the literature reported by Karunaratne et al. [25]. Even the five times difference was too small to interpret the significantly improved γ'' stability (by ~2 orders of magnitude) by replacing Nb with Ta, since a metallurgical principle tells that diffusional transformation kinetics are proportional to the square root of the diffusion coefficient. The reported diffusion coefficients of Ta and V were in the same order, suggesting that the observed improvement in the γ'' stability by the V replacement could not be interpreted by the diffusion kinetics viewpoint.
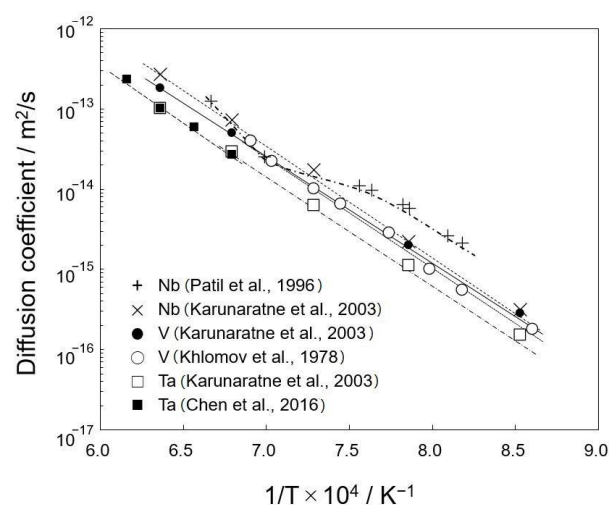

Figure 9. Arrhenius plots for the reported interdiffusion coefficient values of Nb [24,25], V [25,26], and Ta [25,27] in Ni.

4. Conclusions

The effects of alloying elements, M (M = Nb, Ta, and V), on the stability of D0$_{22}$ γ''-Ni$_3$M precipitates at elevated temperatures were investigated in Alloy-718-type Ni-22Cr-based ternary and quaternary alloys using heat-treated diffusion-multiple and bulk samples with discrete chemical compositions. The main results were:

1. The microstructural characterization indicated that a complete replacement of Nb with Ta stabilized the γ'' precipitates at temperatures up to 800 °C.
2. A partial replacement of Ta with V was found to stabilize the precipitates even at 900 °C.
3. Differential scanning calorimetry and high-temperature X-ray diffraction experiments demonstrated that the D0a structure, instead of the D0$_{22}$ structure, was stable at elevated temperatures in the Ni-Cr-Ta ternary system.
4. Lattice parameter measurements suggested that the partial replacement of Ta with V drastically decreased the lattice misfit between the fcc γ matrix and the γ'' precipitate along the two axes of the tetragonal γ'' structure.
5. A consideration of the chemical driving force, misfit strain, and diffusion kinetics viewpoints may qualitatively suggest that either of the former two factors or both could be important factors for the stability of γ'' precipitates at elevated temperatures.

Conflicts of Interest: The authors declare no conflict of interest.

References

1.   INCONEL®Alloy 718, SPECIAL METALS. Available online: www.specialmetals.com (accessed on 18 June 2022).
2.   Stoloff, N.S. *Metals Handbook*; ASM International: Materials Park, OH, USA, 1990; Volume 1, 950p.
3.   Sundraraman, M.; Mukhopadhyay, P.; Banerjee, S. Some aspects of the precipitation of metastable intermetallic phases in Inconel 718. *Metall. Trans. A* **1988**, *19*, 453–465. [CrossRef]
4.   Slama, C.; Abdellaoui, M. Structural characterization of the aged Inconel 718. *J. Alloys Compd.* **2004**, *306*, 277–284. [CrossRef]
5.   Kennedy, R.L. Allvac®718plusTM, Superalloy for the Next Forty Years. In *Superalloys 718, 625, 706 and Various Derivatives*; TMS: Warrendale, PA, USA, 2005; pp. 1–14. 718p.
6.   Collier, J.P.; Song, H.W.; Phillips, J.C.; Tien, J.K. The effect of varying Al, Ti, and Nb content on the phase-stability of Inconel-718. *Metall. Trans.* **1988**, *19*, 1657–1666. [CrossRef]
7.   Mignanelli, P.M.; Jones, N.G.; Pickering, E.J.; Messé, O.M.D.M.; Rae, C.M.F.; Hardy, M.C.; Stone, H.J. Gamma-gamma prime-gamma double prime dual-superlattice superalloys. *Scr. Mater.* **2017**, *136*, 136–140. [CrossRef]
8.   Loewenkamp, S.A.; Radavich, J.F. Microstructure and properties of Ni-Fe base Ta-718. In *Superalloys 1988, Proceedings of the Sixth International Symposium, Champion, PA, USA, 18–22 September 1988*; U.S. Department of Energy: Oak Ridge, TN, USA, 1988; pp. 53–61.
9.   Nash, P.; Nash, A. *Phase Diagrams of Binary Nickel Alloys*; ASM International, The Materials Information Society: Materials Park, OH, USA, 1993.
10. Firstov, G.S.; Koval, Y.N.; Humbeeck, J.V.; Ochin, P. Martensitic transformation and shape memory effect in Ni3Ta: A novel high-temperature shape memory alloy. *Mater. Sci. Eng. A* **2008**, *481–482*, 590–593. [CrossRef]
11. Cozar, R.; Pineau, A. Morphology of γ' and γ'' precipitates and thermal stability of Inconel 718 type alloys. *Metall. Trans. A* **1973**, *4*, 47–59. [CrossRef]
12. Kirman, I. Precipitation in the Fe-Ni-Cr-Nb System. *J. Iron Steel Inst.* **1969**, *207*, 1612–1618.

13. Williams, D.B.; Butler, E.P. Grain boundary discontinuous precipitation reactions. *Int. Met. Rev.* **1981**, *3*, 153–183.
14. Kobayashi, S.; Otsuka, T.; Watanabe, R.; Sagitani, K.; Okamoto, M.; Tokutomi, K. Alloying Effects on the Competition between Discontinuous Precipitation vs. Continuous Precipitation of δ/η Phases in Model Ni Based Superalloys. In *Superalloys 2020, Proceedings of the 14th International Symposium on Superalloys, Online, 13–16 September 2021*; Tin, S., Hardy, M., Clews, J., Cormier, J., Feng, Q., Marcin, J., O'Brien, C., Suzuki, A., Eds.; TMS: Warrendale, PA, USA, 2021; pp. 163–170.
15. Villars, P. *Pearson's Handbook Desk Edition Crystallographic Data for Intermetallic Phases*; ASM International, The Materials Information Society: Materials Park, OH, USA, 1997; Volume 2, p. 2555.
16. Kobayashi, S.; Zaefferer, S. Determination of Phase Equilibria in the Fe3Al-Cr-Mo-C Semi-quaternary System Using a New Diffusion-multiple Technique. *J. Alloys Compd.* **2008**, *452*, 67–72. [CrossRef]
17. Kobayashi, S.; Tsukamoto, Y.; Takasugi, T.; Chinen, H.; Omori, T.; Ishida, K.; Zaefferer, S. Determination of Phase Equilibria in the Co-rich Co–Al–W Ternary System with a Diffusion-Couple Technique. *Intermetalics* **2009**, *17*, 1085–1089. [CrossRef]
18. Kobayashi, S.; Takasugi, T. Mapping of 475 °C embrittlement in ferritic Fe-Cr-Al alloys. *Scripta Mater.* **2010**, *63*, 1104–1107. [CrossRef]
19. Kobayashi, S.; Kimura, K.; Tsuzaki, K. Interphase precipitation of Fe2Hf Laves phase in a Fe-9Cr/Fe-9Cr-Hf diffusion couple. *Intermetallics* **2014**, *46*, 80–84. [CrossRef]
20. Zhou, S.H.; Wang, Y.; Chen, L.Q.; Liu, Z.K.; Napolitano, R.E. Solution-based thermodynamic modeling of the Ni-Ta and Ni-Mo-Ta systems using first principles calculations. *CALPHAD* **2009**, *33*, 631–641. [CrossRef]
21. Zhou, Y.; Wen, B.; Ma, Y.; Melnik, R.; Liu, X. First-principles studies of Ni-Ta intermetallic compounds. *J. Solid State Chem.* **2012**, *187*, 211–218. [CrossRef]
22. Materials Project. Available online: https://materialsproject.org (accessed on 18 June 2022).
23. Cullity, B.D. *Elements of X-ray Diffraction*, 2nd ed.; Agune: Tokyo, Japan, 1979; 332p. (In Japanese)
24. Patil, R.V.; Kale, G.B. Chemical diffusion of niobium in nickel. *J. Nucl. Mater.* **1996**, *230*, 57–60. [CrossRef]
25. Karunaratne, M.S.A.; Reed, R.C. Interdiffusion of the platinum-group metals in nickel at elevated temperatures. *Acta Mater.* **2003**, *51*, 2905–2919. [CrossRef]
26. Khlomov, V.S.; Pimenov, V.N.; Ugaste, Y.E.; Gurov, K.P. Investigation of mutual diffusion in the system Nickel-Vanadium. *Phys. Met. Metallogr.* **1978**, *46*, 188–191.
27. Chen, J.; Xiao, J.; Zhang, L.; Du, Y. Interdiffusion in fcc Ni-X (X = Rh, Ta, W, Re and Ir) alloys. *J. Alloys Compd.* **2016**, *657*, 457–463. [CrossRef]